

^2H -Labeling of Silk Fibroin Fibers and Their Structural Characterization by Solid-State ^2H NMR

Tetsuo Asakura,^{*,†} Masashi Minami,[†] Reiko Shimada,[†] Makoto Demura,[†] Minoru Osanai,[‡] Teruaki Fujito,[§] Mamoru Imanari,[§] and Anne S. Ulrich^{*,||}

Department of Biotechnology, Tokyo University of Agriculture and Technology, Koganei, Tokyo 184, Japan, Department of Biology, Kanazawa University, Kanazawa, Ishikawa 920-11, Japan, JEOL Ltd., Akishima, Tokyo 196, Japan, and Institut fuer Molekularbiologie, Friedrich-Schiller-Universitaet, Jena, Germany

Received November 13, 1996[®]

ABSTRACT: Three kinds of ^2H -labeled *Bombyx mori* silk fibroin samples (with $[2,2\text{-}^2\text{H}_2]\text{Gly}$, $[3,3,3\text{-}^2\text{H}_3]\text{Ala}$, or $[2,3,5,6\text{-}^2\text{H}_4]\text{Tyr}$) were obtained by oral administration of either the labeled amino acid or $^2\text{H}_2\text{O}$ to 5th instar larvae. The administration of $^2\text{H}_2\text{O}$ alone yielded a high degree of selective deuteration at the alanine methyl group, since the incorporation of $^2\text{H}_2\text{O}$ occurs between fumarate and malate in the tricarboxylic acid (TCA) cycle of the silk fibroin synthetic pathway. Uniaxially oriented silk fibers were prepared as samples for ^2H -NMR spectroscopy. An analysis of the quadrupole echo line shape was carried out in order to determine the angle of the deuterium-labeled group relative to the fiber axis, i.e., of the $\text{C}\alpha\text{-}^2\text{H}$ bond vectors in glycine and of $\text{C}\alpha\text{-C}\beta^2\text{H}_3$ in alanine. With the fiber axis aligned parallel to the magnetic field, quadrupole splittings were obtained as 117.8 and 39.8 kHz for $[2,2\text{-}^2\text{H}_2]\text{Gly}$ - and $[3,3,3\text{-}^2\text{H}_3]\text{Ala}$ -labeled silk, respectively. These values are identical with those obtained from the ^2H -NMR powder patterns of the unaligned samples, within experimental error. From the angular dependence of the quadrupole splittings, it was thus calculated that the $\text{C}\alpha\text{-}^2\text{H}$ bonds of glycine as well as the $\text{C}\alpha\text{-C}\beta^2\text{H}_3$ bond of alanine make an angle of approximately 90° relative to the fiber axis. These steric constraints were then used to evaluate the torsion angles, ϕ and ψ , for the glycine and alanine residues within the protein backbone. These data, determined independently by solid-state ^2H NMR, thus verified and narrowed down the allowed region in the Ramachandran (ϕ , ψ) map obtained from previous solid-state ^{13}C - and ^{15}N -NMR studies.

Introduction

Deuterium solid-state NMR has frequently been used during the last decade to characterize the structure and dynamics of polymers, including proteins.^{1–5} The advantage of ^2H NMR for studying a deuterium-labeled polymer is that the line shape and relaxation behavior are determined predominantly by the quadrupolar interaction, which can be up to 250 kHz. Other interactions, such as the deuterium chemical shift or the deuterium–proton and deuterium–deuterium dipolar interactions, are about 100 times less in magnitude. The coupling between the deuterium nuclear quadrupole moment and the electric field gradient at the nucleus is a direct reflection of the local electron distribution in a particular bonding arrangement. The quadrupole splitting can thus be analyzed to yield the orientational angle of a labeled group in a uniaxially aligned sample, provided that the bond vector is immobile on the NMR time scale or undergoes restricted anisotropic motion.

^2H -NMR spectroscopy is being applied here to the structural analysis of a fibrous protein, *Bombyx mori* silk fibroin. A major part of its amino acid sequence has been recently traced by genetic engineering techniques.⁶ The overall composition in mol % consists of glycine (42.9%), alanine (30.0%), serine (12.2%), tyrosine (4.8%), and valine (2.5%), and the predominant sequence is a repeating motif of six amino acids ($\text{Gly-Ala-Gly-Ala-Gly-Ser}$)_n.⁷ The backbone structure of silk fibroin fiber was shown to be an antiparallel β -sheet. In particular, ^{13}C and ^{15}N CP/MAS NMR studies^{8–11} provided such evidence on the basis of conformation-

dependent chemical shifts and orientation-dependent interactions of uniaxially aligned $[^{15}\text{N}]$ - and $[1\text{-}^{13}\text{C}]$ -labeled fiber samples.^{12–15} The structural conclusions from solid-state NMR are in agreement with the results from IR studies,⁹ X-ray diffraction,^{9,16,17} and conformational energy calculations.¹⁸

In a previous report¹⁹ we have analyzed the ^2H -NMR powder patterns of $[3,3\text{-}^2\text{H}_2]\text{Ser}$ - and $[3,3,3\text{-}^2\text{H}_3]\text{Ala}$ -labeled silk fibroin. The respective side-chain mobilities can be interpreted in terms of their structural stabilization in the immobilized protein. The reorientation of most of the serine residues is virtually frozen, while the methyl group of alanine undergoes rapid 3-fold rotation about the $\text{C}\alpha\text{-C}\beta$ axis. This suggests that the hydroxyl groups might be attached to carbonyl or amide groups via intra- or interchain hydrogen bonds. Simmons et al.²⁰ recorded solid-state ^2H -NMR spectra of $[3,3,3\text{-}^2\text{H}_3]\text{Ala}$ -labeled spider dragline silk and analyzed its detailed relaxation behavior. From the two kinds of relaxation times obtained, they concluded that about 40% of the alanine methyl groups are present in β -sheets that are well oriented along the fiber axis. The other 60% are poorly oriented, with a large volume available for unimpeded methyl reorientation. These ^2H -NMR studies were mainly concerned with the dynamics in silks.

In the study presented here, we use solid-state ^2H NMR of oriented samples to determine details of the silk fibroin structure with quasi-atomic resolution. Various ^2H -labeled silk fibroin samples are prepared by the oral administration of isotope-labeled amino acids or $^2\text{H}_2\text{O}$ to 5th instar larvae.^{8–15,21–26} The spectral line shape of the uniaxially aligned fibers is analyzed to give the relative orientation of the deuterated group with respect to the fiber axis for $[2,2\text{-}^2\text{H}_2]\text{Gly}$ and $[3,3,3\text{-}^2\text{H}_3]\text{Ala}$.

[†] Tokyo University of Agriculture and Technology.

[‡] Kanazawa University.

[§] JEOL Ltd.

^{||} Friedrich-Schiller-Universitaet.

[®] Abstract published in *Advance ACS Abstracts*, April 1, 1997.

Ala. The ^2H -NMR data are used as complementary information to narrow down the backbone conformations of glycine and alanine that were calculated from previous solid-state ^{15}N - and ^{13}C -NMR studies of labeled silk fibers.^{13–15} The solid-state ^2H -NMR spectra of a uniaxially aligned $[2,3,5,6\text{-}^2\text{H}_4]\text{Tyr}$ -labeled silk fiber are also analyzed here to obtain information about the orientation of the aromatic tyrosine ring and the dynamics of the ring flip.

Materials and Methods

^2H -Labeling of Silk Fibroin. *Bombyx mori* larvae of hybrids of a commercial stock, Shuko \times Ruhuaku, were reared with an artificial diet (Silk Mater, 1S and 2S, Nihon Nosan Kogyo Co., Tokyo, Japan) at 25 $^\circ\text{C}$.^{19,22} A total of 20 mg of $[2,2\text{-}^2\text{H}_2]\text{Gly}$ (98 atom %, Cambridge Isotope Lab., Andover, MA) was dissolved in water and mixed with 2.7 g of the artificial diet. This was fed to 5th instar silkworms larvae from day 4 to day 8. The $[2,2\text{-}^2\text{H}_2]\text{Gly}$ -labeled silk fibroin was obtained in the form of cocoons. Similarly, $[3,3,3\text{-}^2\text{H}_3]\text{Ala}$ (99 atom %, Masstrace Inc., Woburn, MA) and $[2,3,5,6\text{-}^2\text{H}_4]\text{Tyr}$ (98 atom %, Cambridge Isotope Lab., Andover, MA) were used in this study. As an alternative route of labeling, 0.05 mL/day of pure $^2\text{H}_2\text{O}$ was orally administered to 5th instar silkworms from day 4 to day 8.

In order to check the degree of ^2H incorporation, representative labeled samples were dissolved in trifluoroacetic acid (TFA) at a concentration of 7.0 w/v %. Solution-state ^2H -NMR spectra were recorded on a JEOL FX-90Q NMR spectrometer operating at 13.7 MHz. Since silk fibroin has a random-coil conformation in TFA, all ^2H nuclei in the labeled protein could be observed. Only those types of silk fibroin samples were used for the subsequent solid-state ^2H NMR experiments that had a sufficiently high and selective labeling ratio.

Preparation of Uniaxially Aligned Samples of ^2H -Labeled Silk Fibers. The silk fibroin fibers for solid-state ^2H -NMR measurements were prepared by first loosening the threads of the cocoons by placing them in 100 $^\circ\text{C}$ water for 5 min.^{10,13} The ends of the cocoon fibers were located, bundled together, and wound onto a glass tube. In order to remove silk sericin, the silk fibers on the glass tube were boiled in a 0.5 w/v % Marseilles soap solution for 30 min and then washed with distilled water. Thin sheets of the uniformly aligned fibers were prepared with a quick-setting bonding agent and cut into 4.5×12 mm pieces. These sheets were then stacked together and fixed with the bonding agent to form a $4.5 \times 4.5 \times 12$ mm block which fits into the radio-frequency coil of the NMR probe.²⁷

Solid-State ^2H -NMR Experiments. ^2H -NMR spectra of both the aligned and the unaligned ^2H -labeled silk fibers were recorded at 61.25 MHz on a JEOL GX-400 NMR spectrometer equipped with a solid-state ^2H -NMR unit. The quadrupole echo pulse sequence ($90^\circ_x - \tau - 90^\circ_y - \tau - \text{echo}$) was used, with an interval $\tau = 34$ μs and 90° pulses of 3.4 μs . The recycle delay was 1.0 s for $[2,2\text{-}^2\text{H}_2]\text{Gly}$ -labeled silk fibroin, 0.5 s for $[3,3,3\text{-}^2\text{H}_3]\text{Ala}$, and 0.1 s for $[2,3,5,6\text{-}^2\text{H}_4]\text{Tyr}$ -labeled samples. All NMR experiments were performed at room temperature. The angle α between the axis of the uniaxially aligned fiber block and the static magnetic field could be varied by rotating the sample in the NMR tube manually.¹² The number of accumulations was 5000 for $[2,2\text{-}^2\text{H}_2]\text{Gly}$ -labeled silk fibroin and 80 000 for $[3,3,3\text{-}^2\text{H}_3]\text{Ala}$ - and $[2,3,5,6\text{-}^2\text{H}_4]\text{Tyr}$ -labeled samples.

^2H -NMR Theory and Analysis. The quadrupole splitting $\Delta\nu_Q$ of an aliphatic deuteron is determined by the angle θ between the C– ^2H bond vector and the static magnetic field direction B_0 , according to^{2,4,5,29,30}

$$\Delta\nu_Q = (3/4)(e^2qQ/h)(3\cos^2\theta - 1) \quad (1)$$

where $e^2qQ/h = 168$ kHz is the rigid lattice quadrupole coupling constant and the asymmetry parameter is assumed to be zero. When all deuterium bonds in the sample are aligned in the same direction with respect to the magnetic field, the resulting spectrum will consist of a pair of narrow

lines. Such uniaxial geometry is characteristic of fibers that are aligned parallel to the magnetic field direction. In that case, all deuterium bond vectors lie along the rim of a cone around the fiber axis, and the cone angle is equivalent to θ . It is thus possible to determine the molecular bond vector relative to the fiber axis directly from the measured quadrupole splitting $\Delta\nu_Q$, using eq 1. For values of θ greater than 35° , however, there exist two redundant solutions, since positive and negative signs of $\Delta\nu_Q$ cannot be discriminated from the spectral splitting alone.

An unoriented sample is described by a different kind of geometry, since the deuterium bond vectors are statistically distributed over all orientations in space. Each angle θ between 0° and 90° contributes a different quadrupole splitting to the resulting powder pattern, which consists of the weighted sum over all orientations. The most prominent peaks in the characteristic powder lineshape represent the deuterium bond vectors aligned at 90° relative to the magnetic field. The peak separation will be referred to as the powder splitting, $\Delta\nu_{Q(\text{powder})}$. For a rigid powder sample its value is about 126 kHz according to the equation above.

A third, intermediate kind of line shape is observed when a fiber is tilted at an angle α relative to the static magnetic field.^{30–33} The deuterium bond vectors are aligned symmetrically around the fiber axis and are therefore distributed over a range of different angles θ relative to the magnetic field. Due to the limited set of values for θ , the resulting line shapes are relatively complex, with two or more maxima. By analyzing the line shapes of tilted fiber samples, it is possible to discriminate between positive and negative values of $\Delta\nu_Q$ and to resolve any redundant solutions for θ that were calculated from eq 1.³¹

Generally, the effect of molecular motion is to reduce the quadrupole coupling to a time-averaged value which is smaller than the rigid lattice constant. For example, the fast rotation of a methyl group around its well-defined tetrahedral angle scales down the total width of the line shape by a factor of 3. At room temperature, even a restricted bond may undergo some small-amplitude random oscillations that are fast on the ^2H -NMR time scale. In that case, the apparent powder splitting will be slightly narrower than the expected rigid lattice of 126 kHz. Line-shape analysis of the spectra was carried out by computer simulation, to determine those angles and line-broadening parameters that produce the best fit to the experimental data. Details of the simulation procedure for oriented ^2H -NMR spectra are described elsewhere by Ulrich et al.^{30–32} Briefly, the intrinsic (Lorentzian) line-width parameter is determined first, by simulating the powder pattern independently. With this value, a set of line shapes is then generated for the oriented spectra at the different tilt angles α . In a concerted series of steps the unique angle for the deuterium bond vector is optimized to fit the whole tilt series. The simulation program also allows an estimation of the (Gaussian) mosaic spread, by optimizing this parameter in a similar way. The static disorder of α around the axis of orientation accounts for most of the effective line width of the oriented spectra, since the fibers are not perfectly aligned.

Results

^2H Incorporation into *B. mori* Silk Fibroin. Figure 1 shows the ^2H -NMR spectra of various ^2H -labeled silk fibroins dissolved in TFA. These samples were obtained by oral administration of either (A–C) isotope-labeled amino acids or (D) $^2\text{H}_2\text{O}$ to the silkworm. The natural-abundance COO^2H peak of TFA was used as a chemical shift reference and assumed to be 11.3 ppm from TMS.²⁸ The intensity of this peak served as a reference to estimate the degree of ^2H incorporation. There was essentially no natural-abundance ^2H background from silk fibroin under the experimental conditions used. The resonances of the labeled silk fibroins were readily assigned on the basis of the chemical shifts of the pure ^2H -labeled amino acid in TFA, and the peaks are marked by arrows in Figure 1.

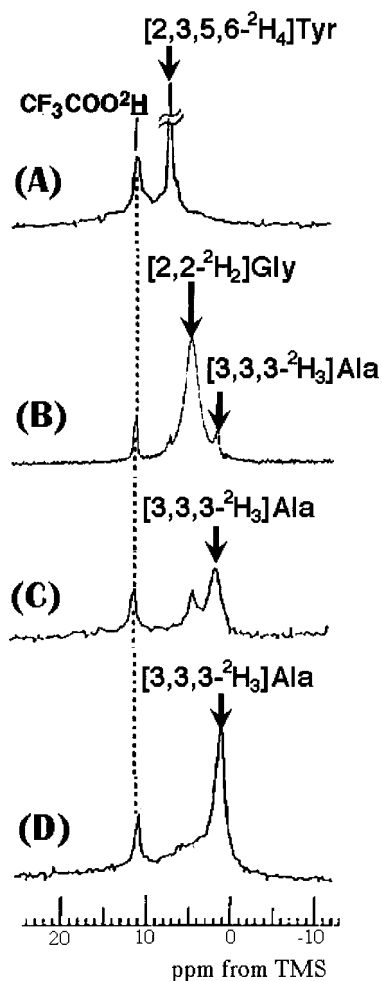


Figure 1. Solution ^2H -NMR spectra of ^2H -labeled silk fibroin dissolved in trifluoroacetic acid (TFA). Samples A–C were obtained from cocoons after rearing the silkworm with an artificial diet containing added ^2H -labeled amino acids: (A) $[2,3,5,6\text{-}^2\text{H}_4]\text{Tyr}$, (B) $[2,2\text{-}^2\text{H}_2]\text{Gly}$, and (C) $[3,3,3\text{-}^2\text{H}_3]\text{Ala}$. Sample D was obtained after injection of $^2\text{H}_2\text{O}$ into the silkworm. The chemical shift of the natural-abundance TFA COO^2H peak is assumed to be 11.3 ppm from TMS.

In spectrum 1A of $[2,3,5,6\text{-}^2\text{H}_4]\text{Tyr}$ -labeled silk fibroin, only one sharp peak at around 7 ppm is observed besides the TFA signal, which is assigned to the aromatic tyrosine ring. It is thus likely that any metabolic pathways from tyrosine to other amino acids, at least from the aromatic ring, can be neglected.²¹ The ^2H intensity of the $[2,3,5,6\text{-}^2\text{H}_4]\text{Tyr}$ peak is 2.5 times higher than that of TFA.

In the case of $[2,2\text{-}^2\text{H}_2]\text{Gly}$ - and $[3,3,3\text{-}^2\text{H}_3]\text{Ala}$ -labeled silk fibroins, it is apparent that some metabolic pathways in the silkworm can convert glycine and alanine into other amino acids, judging by the appearance of additional peaks in spectra 1B and 1C. In spectrum 1B, a small peak at around 1.5 ppm is observed next to the main peak of $[2,2\text{-}^2\text{H}_2]\text{Gly}$ at around 4 ppm. The small peak is assigned to a deuterated alanine methyl group according to its chemical shift known from the $[3,3,3\text{-}^2\text{H}_3]\text{Ala}$ spectrum 1C. It is thus concluded that some metabolic transfer from $[2,2\text{-}^2\text{H}_2]\text{Gly}$ to alanine occurs in the silkworm. The intensity of the $[2,2\text{-}^2\text{H}_2]\text{Gly}$ peak is 7.5 times higher than that of TFA.

Spectrum 1C contains an additional peak at around 3.8 ppm besides the solvent and the main $[3,3,3\text{-}^2\text{H}_3]\text{Ala}$ signal. This additional peak is assigned to the methylene group of serine according to its chemical shift

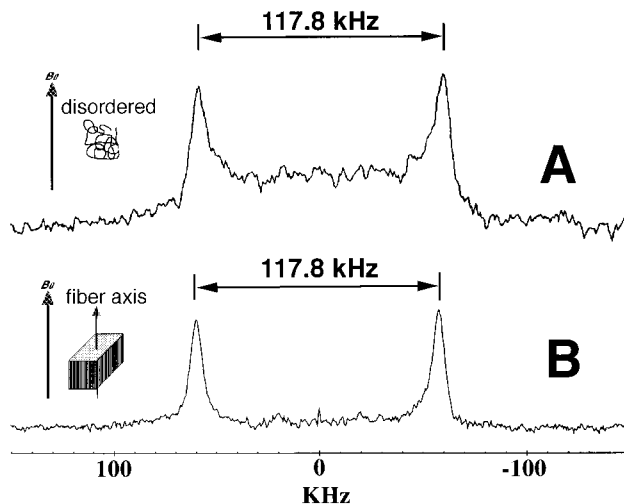


Figure 2. Solid-state ^2H NMR quadrupole echo spectra of (A) unaligned $[2,2\text{-}^2\text{H}_2]\text{Gly}$ -labeled silk fiber and (B) a uniaxially aligned sample where the fiber axis was set parallel to the magnetic field direction, B_0 ($\alpha = 0^\circ$). Each spectrum was obtained at room temperature from 5000 accumulations.

value known from previous studies.¹⁹ The peak intensity is comparable to that of TFA, which indicates that a significant degree of transfer occurs from $[3,3,3\text{-}^2\text{H}_3]\text{Ala}$ to serine. This sample, prepared by directly feeding $[3,3,3\text{-}^2\text{H}_3]\text{Ala}$ to the silkworm, is thus not suitable for the solid-state ^2H -NMR analysis presented here. However, it was found that when feeding the silkworm with pure $^2\text{H}_2\text{O}$ instead, a much improved sample with a selectively labeled alanine methyl group can be obtained, as shown in Figure 1D. The chemical shift of the main peak is 1.5 ppm, which is in agreement with the chemical shift of the $[3,3,3\text{-}^2\text{H}_3]\text{Ala}$ methyl peak in Figure 1C. Its intensity is 4.7 times higher than the solvent signal. The main peak is broadened by an underlying signal at its low-field side, indicating the production of some other amino acids from $^2\text{H}_2\text{O}$, which is, however, negligible compared to the situation in spectrum 1C. This type of sample (D) with an improved degree of selective ^2H labeling is thus used to investigate the structure of alanine in silk fibers by solid-state ^2H NMR.

The possible metabolic pathway from $^2\text{H}_2\text{O}$ into the alanine methyl group will be considered later in the Discussion section. In our previous work, various silk fibroins with a high ^{15}N isotope labeling ratio for glycine, alanine, or tyrosine were obtained by a different method of cultivating the isolated silk gland.^{15,25} We have therefore also tried to obtain ^2H -labeled samples by this method, using a medium with deuterated amino acids; however, no satisfactory ^2H labeling could be achieved that way.

^2H -NMR Spectra of $[2,2\text{-}^2\text{H}_2]\text{Gly}$ -Labeled Silk Fibroin. Figure 2A shows the solid-state ^2H -NMR powder pattern of unaligned $[2,2\text{-}^2\text{H}_2]\text{Gly}$ -labeled silk fibroin. The splitting of $\Delta\nu_Q = 117.8$ kHz is slightly smaller than the expected rigid-lattice value of about 126 kHz. This indicates that the methylene group of the glycine residue is essentially restricted in space and undergoes only some small-amplitude vibrational motion at room temperature. This conclusion is in agreement with the prediction from the intermolecular hydrogen bonding network in the silk fibroin backbone with an antiparallel β -sheet conformation. Since the experimentally determined powder splitting represents the effective coupling constant at room temperature, eq

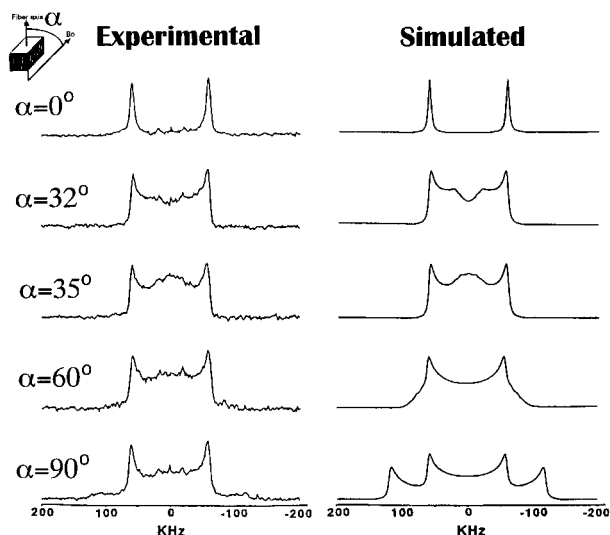


Figure 3. Experimental and simulated ^2H -NMR spectra of uniaxially aligned $[2,2\text{-}^2\text{H}_2]\text{Gly}$ -labeled silk fibers, where the angle α between the fiber axis and magnetic field was set to 0° , 32° , 35° , 60° , and 90° . The experimental spectra on the left compare well with the simulated line shapes on the right, for which the angle θ between the $\text{C}\alpha\text{-}^2\text{H}_2$ bond vector and the fiber axis was assumed to be 90° .

1 needs to be scaled proportionally. The time average $\langle 3/4e^2qQ/h \rangle = 117.8$ kHz will be thus used, instead of 126 kHz, in order to calculate the value of θ from the oriented spectrum below.

Figure 2B shows the ^2H -NMR spectrum of the uniaxially aligned $[2,2\text{-}^2\text{H}_2]\text{Gly}$ -labeled silk sample, with the fiber axis set parallel to the magnetic field direction. Only a single pair of resonances is observed in the oriented spectrum for the two $\text{C}\alpha\text{-}^2\text{H}$ bonds of glycine, which indicates that both bonds lie at the same angle with the fiber axis. Their respective orientations could either be aligned in parallel or be pointing above and below the perpendicular plane of the fiber. A comparison of the oriented spectrum 2B with the corresponding powder spectrum in Figure 2A shows that these different geometries exhibit an identical splitting of $\Delta\nu_Q = 117.8$ kHz. The angle of the $\text{C}\alpha\text{-}^2\text{H}$ bond vectors in glycine is calculated using the proportionally scaled eq 1. Two possible solutions are obtained, with $\theta = 90^\circ$ or 35° depending on the sign of the quadrupole splitting. By taking into account an experimental error of ± 0.2 kHz, the angle is calculated as $90^\circ \pm 3^\circ$ or $35^\circ \pm 0.5^\circ$.

In order to discriminate between the two possible solutions, ^2H -NMR spectra of the uniaxially oriented $[2,2\text{-}^2\text{H}_2]\text{Gly}$ sample were recorded as a function of the tilt angle α between the fiber axis and B_0 . A tilt series of these spectra is shown in Figure 3 along with the line-shape simulations performed for the case of $\theta = 90^\circ$. Simulations were carried out with an intrinsic line-width parameter of 2 kHz, and a mosaic spread of $\pm 5^\circ$ was found to reproduce the experimental data best. The agreement between the observed and simulated spectra is good, which confirms the result of 90° . When the tilt angle deviates from $\alpha = 0^\circ$ (where the fiber axis is parallel to B_0), the intensity between the peaks increases, and the line shape is very sensitive near $\alpha = 30^\circ$. When α approaches 90° , a set of wings appear, which have a somewhat weaker intensity than predicted. It is likely that this reduction in intensity is due to a nonlinear excitation profile of the ^2H pulse across the very large spectral width.

^2H -NMR Spectra of $[3,3,3\text{-}^2\text{H}_3]\text{Ala}$ -Labeled Silk Fibroin. Figure 4A shows the ^2H -NMR powder pattern

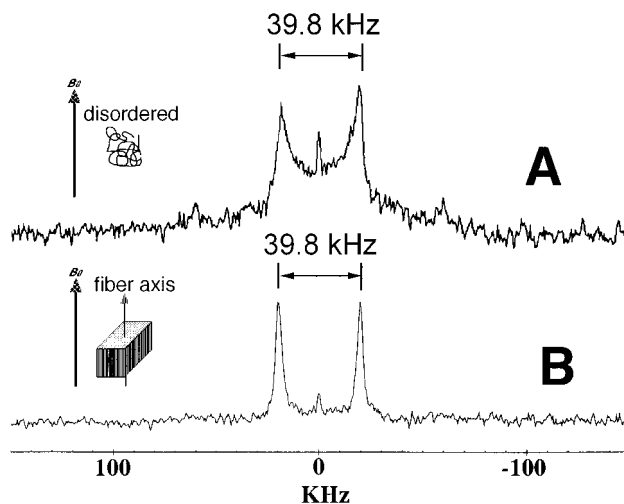


Figure 4. Solid-state ^2H -NMR spectra of (A) unaligned $[3,3,3\text{-}^2\text{H}_3]\text{Ala}$ -labeled silk fibroin fibers and (B) a uniaxially aligned sample where the fiber axis was set parallel to the magnetic field direction, B_0 ($\alpha = 0^\circ$). Each spectrum was acquired at room temperature with 80 000 accumulations.

of $[3,3,3\text{-}^2\text{H}_3]\text{Ala}$ -labeled silk fibroin and underneath the corresponding spectrum of the oriented fiber sample at $\alpha = 0^\circ$. Both sample geometries give rise to the same splitting of $\Delta\nu_Q = 39.8$ kHz, within experimental error. The value of the powder splitting indicates a fast 3-fold rotation of the alanine methyl group about its $\text{C}\alpha\text{-C}\beta$ axis, as reported previously.¹⁹ This is also in agreement with the minimum in the spin-lattice relaxation time T_1 , which was observed between -70 and -80°C in a ^1H -NMR study of *B. mori* silk fibroin at 90 MHz.³⁴ A small additional doublet with $\Delta\nu_Q = 118$ kHz is seen in spectrum 4A, due to the presence of a small amount of labeled glycine or serine, which is produced by feeding with $^2\text{H}_2\text{O}$ as seen in Figure 1A. If the contribution arises from labeled serine, the signal corresponds to the $\text{C}\beta\text{-}^2\text{H}_2$ bonds of the side chain which is hydrogen bonded to C=O or NH groups.¹⁹ The single center peak is due to H^2HO .

Using the powder splitting from unaligned $[3,3,3\text{-}^2\text{H}_3]\text{Ala}$ -labeled silk fibroin as the reference for eq 1, the angle of the $\text{C}\alpha\text{-C}\beta$ bond vector of alanine was calculated to be either 90° or 35° with respect to the fiber axis.³⁰⁻³² The correct value of θ was resolved by changing the sample tilt angle from $\alpha = 0^\circ$ to 90° . Figure 5 shows a comparison between the experimental data and the corresponding line shapes that were simulated for the two possible cases of $\theta = 35^\circ$ and 90° , with an intrinsic line width of 2 kHz and a mosaic spread of $\pm 7^\circ$. The simulated line shape (at $\alpha = 90^\circ$) for the case of $\theta = 35^\circ$ does not fit the experimental spectrum, but if θ is assumed to be 90° , there is very good agreement. With an experimental error of ± 0.2 kHz, the angle of the $\text{C}\alpha\text{-C}\beta^2\text{H}_3$ bond vector of alanine is thus determined to be $\theta = 90^\circ \pm 3^\circ$ with respect to the fiber axis.

^2H -NMR Spectra of Oriented $[2,3,5,6\text{-}^2\text{H}_4]\text{Tyr}$ -Labeled Silk Fiber. Figure 6 shows the ^2H -NMR spectra of the block of uniaxially aligned $[2,3,5,6\text{-}^2\text{H}_4]\text{Tyr}$ -labeled silk, with the fiber axis parallel ($\alpha = 0^\circ$) and perpendicular ($\alpha = 90^\circ$) to B_0 . Besides the central $^2\text{H}_2\text{O}$ peak, two doublets are observed for either sample alignment, which display a slight dependence on the tilt angle. The inner doublet appears to reflect fast 180° flips about the $\text{C}\beta\text{-C}\gamma$ axis,^{1-3,35} with a quadrupole splitting of 38.0 kHz ($\alpha = 0^\circ$) or 35.8 kHz ($\alpha = 90^\circ$).

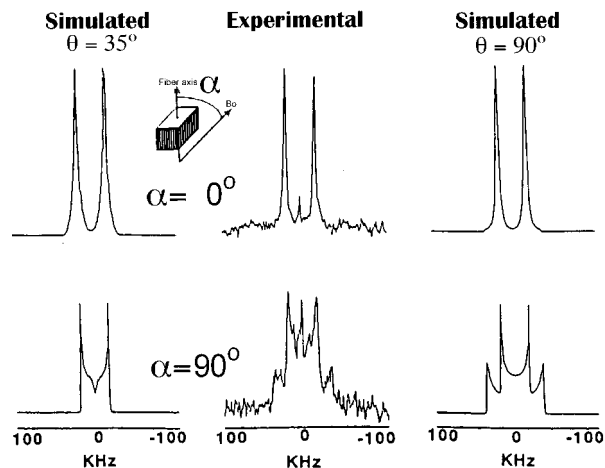


Figure 5. Experimental and simulated ^2H -NMR spectra of uniaxially aligned $[3,3,3\text{-}^2\text{H}_3]\text{Ala}$ -labeled silk fibroin, where the fiber axis was set parallel ($\alpha = 0^\circ$) and perpendicular ($\alpha = 90^\circ$) to the magnetic field direction, B_0 . The experimental spectra are shown in the middle column, for comparison with the simulated line shapes on either side. For the simulations on the left, the angle θ between the alanine $\text{C}\alpha\text{-C}\beta^2\text{H}_3$ bond and the fiber axis was assumed to be 35° and on the right 90° .

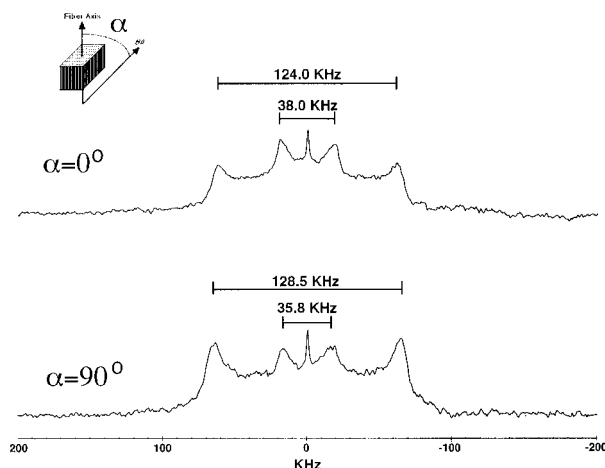


Figure 6. ^2H -NMR spectra of uniaxially aligned $[2,3,5,6\text{-}^2\text{H}_4]\text{Tyr}$ -labeled silk fibroin, where the fiber axis was set parallel ($\alpha = 0^\circ$) and perpendicular ($\alpha = 90^\circ$) relative to the magnetic field direction B_0 , at room temperature.

The outer doublet displays a splitting of 124.0 kHz ($\alpha = 0^\circ$) or 128.5 kHz ($\alpha = 90^\circ$). These orientation-dependent spectra thus indicate that there are still immobile components on the NMR time scale, or components with restricted anisotropic motion, even in the presence of fast 180° flips.³⁶ A structural analysis for tyrosine is in progress, but it is complicated by the effects of motion, by the additional torsion angles of the flexible side chain (compared to glycine and alanine), and by the presence of two discrete $^2\text{H}_2$ bond orientations in the ring (as in the case of glycine).

Discussion

Metabolic Pathways and ^2H Labeling of Silk Fibroin. The $[2,2\text{-}^2\text{H}_2]\text{Gly}$ - and $[2,3,5,6\text{-}^2\text{H}_4]\text{Tyr}$ -labeled silk fibroin samples for the solid-state ^2H -NMR study could be prepared with a high degree of deuteration by feeding the corresponding isotope-labeled amino acid to the silkworm. In order to achieve a high degree of alanine labeling, however, the administration of $^2\text{H}_2\text{O}$ to the silkworm proved to be more effective than feeding with $[3,3,3\text{-}^2\text{H}_3]\text{Ala}$. The metabolic pathway from $^2\text{H}_2\text{O}$ to alanine in the silkworm thus needs to be discussed

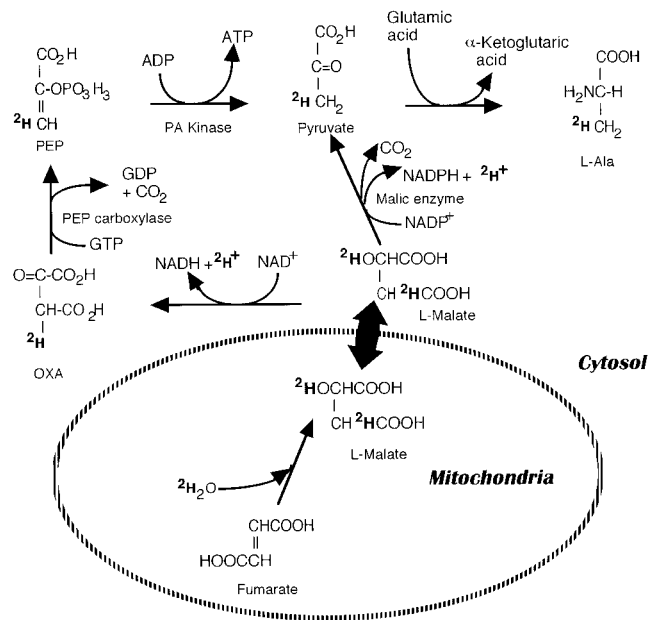


Figure 7. Possible metabolic pathway of how $^2\text{H}_2\text{O}$ injected into the silkworm is incorporated into the alanine methyl group. Details and abbreviations are described in the text.

in detail.^{7,23,37} There is no possibility of $^2\text{H}_2\text{O}$ incorporation into the intermediates during glycolysis. Therefore, the TCA cycle is considered to be the only process when $^2\text{H}_2\text{O}$ can enter the biosynthetic pathway of silk fibroin. There are two possible stages at which $^2\text{H}_2\text{O}$ can be involved, that is, when either (a) citrate synthetase or (b) fumarate hydratase participate. In the first case (a) one deuteron of $^2\text{H}_2\text{O}$ would be incorporated into the citrate molecule and another one into CoA. However, if the deuterated carboxylate group dissociates, the deuteron would be released. Thus, it is unlikely that $^2\text{H}_2\text{O}$ is incorporated into silk fibroin via the action of citrate synthetase.

Figure 7 illustrates the metabolic pathways involved in the other possibility (b), where $^2\text{H}_2\text{O}$ is incorporated by the catalysis of fumarate hydratase. Glycolysis, which involves pyruvate (PA), takes place in the cytosol of cells, whereas the TCA cycle occurs within the mitochondria. The PA, alanine, and L-malate molecules can pass freely through the mitochondrial membrane, but oxaloacetic acid (OXA) cannot. Therefore, L-malate enters the mitochondrion and is converted into PA. At this point, PA can be produced during gluconeogenesis via OXA and phosphoenol pyruvate (PEP) by catalysis of malate dehydrogenase. Through the action of PEP carboxylase, one deuteron from $^2\text{H}_2\text{O}$ is incorporated into PEP and finally ends up in the methyl group of alanine, which is derived from PA by alanine-pyruvate aminotransferase. Similarly, PA can be formed directly from L-malate by catalysis of the malic enzyme. Also in this case, one deuteron of the alanine methyl group becomes labeled. Therefore, we propose that, as summarized in Figure 7, the alanine methyl group will be labeled by administration of $^2\text{H}_2\text{O}$ to the silkworm.

Torsion Angles of Glycine in Silk Fibers from ^2H NMR. In a previous study,¹³ we have used solid-state ^{15}N NMR of uniaxially aligned $[^{15}\text{N}]\text{Gly}$ -labeled silk fibers to determine the angle of the N-H or N-C bonds relative to the fiber axis. Additionally, the $^{15}\text{N}\text{-}^1\text{H}$ dipolar interaction was employed to narrow down the number of unique orientations. We have also analyzed a uniaxially aligned sample of $[1\text{-}^{13}\text{C}]\text{Gly}$ -labeled silk to determine the angle between the C=O

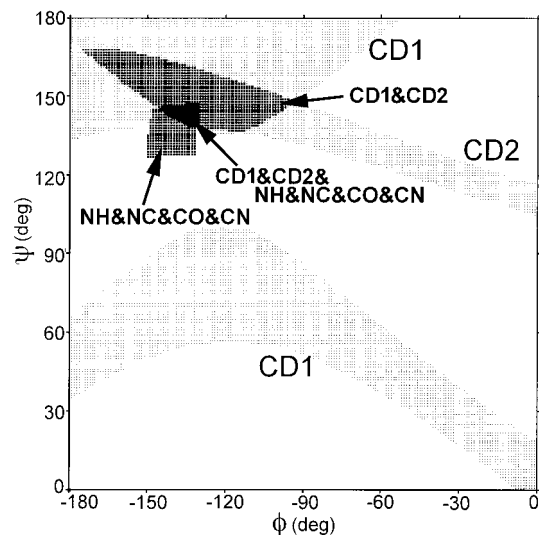


Figure 8. Ramachandran plot of the allowed torsion angles (ϕ and ψ) of glycine in silk fibroin, as determined by solid-state ^{13}C , ^{15}N , and ^2H NMR of uniaxially aligned silk fibers. The area NH&NC&CO&CN corresponds to the respective angles of the bond vectors relative to the fiber axis, as obtained from previous ^{15}N - and ^{13}C -NMR studies. The two curves CD1 and CD2 represent the $\text{C}\alpha\text{--}^2\text{H}_2$ bond vectors of glycine determined here by ^2H NMR.³⁴ The width of the curves represents the experimental error.

or C–N bond vector and the fiber axis.¹⁵ All these observations are in good agreement with the models for the silk II antiparallel β -sheet structure proposed by Marsh et al.,¹⁶ Takahashi et al.,¹⁷ and Fossey et al.¹⁸ With the combined data of these previous studies, the restricted (ϕ , ψ) region for the glycine residue has been calculated in the Ramachandran map ($-180^\circ < \phi < 0^\circ$, $0^\circ < \psi < 180^\circ$) and is shown as the shaded area (NH&NC&CO&CN) in Figure 8.

The ^2H -NMR analysis of uniaxially aligned [2,2- $^2\text{H}_2$]-Gly-labeled silk fibroin fiber has yielded an angle of $\theta = 90 \pm 3^\circ$ for the two glycine $\text{C}\alpha\text{--}^2\text{H}$ bond vectors relative to the fiber axis. The restricted (ϕ , ψ) region for glycine in the Ramachandran map is thus calculated from these new ^2H NMR data and used to narrow down the orientational constraints from our previous results. The experimental curves from the two $\text{C}\alpha\text{--}^2\text{H}$ (CD1 and CD2) bond orientations of glycine are shown in the Ramachandran plot in Figure 8. The width of these curves corresponds to the experimental error of $\pm 3^\circ$ in the determination of θ from the quadrupole splitting. The area of overlap between the two curves covers the antiparallel β -sheet region. The additional constraints from the previous ^{15}N - and ^{13}C -NMR analysis of glycine (NH&NC&CO&CN) overlap within a well-defined area in the allowed (CD1&CD2) region, which is in excellent agreement with the proposed antiparallel β -sheet structure of silk fibroin. The orientational constraints from solid-state ^2H NMR can thus be used effectively to narrow down the allowed region from other ^{13}C - and ^{15}N -NMR studies.

Torsion Angles of Alanine in Silk Fibers from ^2H NMR. From the ^2H -NMR quadrupole splitting $\Delta\nu_Q = 39.8$ kHz, of uniaxially aligned [3,3,3- $^2\text{H}_3$]-Ala-labeled silk fibroin, the angle θ of the $\text{C}\alpha\text{--}^2\text{H}_3$ bond vector of alanine has been calculated as $90 \pm 3^\circ$ relative to the fiber axis. This result is used to determine the torsion angles (ϕ and ψ) of alanine in silk fibroin fibers, to complement our previous solid-state NMR studies.^{14,15} Uniaxially aligned [1- ^{13}C]-Gly-[^{15}N]-Ala silk fibroin fi-

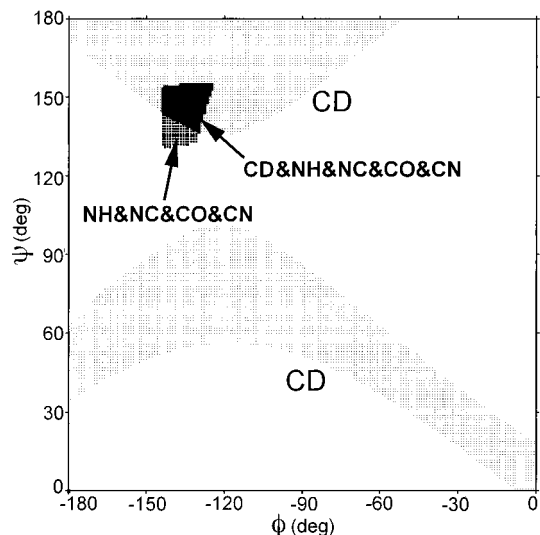


Figure 9. Ramachandran plot of the allowed torsion angles (ϕ and ψ) of alanine in silk fibroin, as determined by solid-state ^{13}C , ^{15}N , and ^2H NMR of uniaxially aligned silk fibers. The area NH&NC&CO&CN corresponds to the angles of the respective bond vectors relative to the fiber axis, as obtained from previous solid-state ^{15}N - and ^{13}C -NMR studies. Curve CD represents the $\text{C}\alpha\text{--}^2\text{H}_3$ bond vector of the alanine methyl group as observed here by ^2H NMR. The width of the curves represents the experimental error.

bers have been obtained by cultivation of the middle silk gland in an amino acid medium containing both [1- ^{13}C]-Gly and [^{15}N]-Ala¹². By ^{15}N NMR, the $^{13}\text{C}\text{--}^{15}\text{N}$ coupling constant was found to be 1.08 ± 0.08 kHz, which yielded an angle of 39° (or 141°) $\pm 2^\circ$ between the $^{13}\text{C}\text{--}^{15}\text{N}$ peptide bond of alanine relative to the fiber axis. Further information about the orientations of the peptide planes in oriented samples was obtained from the chemical shift tensors of ^{15}N and the ^{13}C -carbonyl.¹⁵ The shaded area (NH&NC&CO&CN) in Figure 9 represents the allowed region for alanine in the Ramachandran map, as determined by solid-state ^{15}N and ^{13}C NMR of silk. The additional curve CD from the present ^2H -NMR study was calculated from the angle $\theta = 90 \pm 3^\circ$ of the $\text{C}\alpha\text{--}^2\text{H}_3$ bond vector. The region of overlap between all orientational constraints is obtained in the antiparallel β -sheet region, in excellent agreement with the model for silk fibroin.

The solid-state ^2H -NMR spectra of uniaxially aligned silk fibers reflect the local structure directly via the ^2H quadrupole splitting. In combination with supplementary ^{15}N - and ^{13}C -NMR data, these measurements can thus be used to determine precise backbone and side-chain conformations at any specific site. The excellent fibrous character of silk is attributed to both the crystalline and amorphous regions, which can be discriminated by their respective dynamics. Since the ^2H -NMR line shape contains information about both the structure and the dynamics, these studies may help to understand the origin of the high tensile strength of silk.

Acknowledgment. T.A. acknowledges support from Grant-in-Aid of the Ministry of Education, Science and Culture of Japan (Grant No. 06044075), Yazaki Science Foundation, Japan, Ogasawara Foundation for the Promotion of Science & Engineering, Japan, and the International Human Frontier of Science Program. A.U. gratefully acknowledges the EMBO Foundation and the Fonds der Chemischen Industrie for financial support.

References and Notes

- (1) Jelinski, L. W. In *High Resolution NMR Spectroscopy of Synthetic Polymers in Bulk*; Komoroski, R. A., Ed.; VCH: Weinheim, Germany, 1986; pp 335–363.
- (2) Rice, D. M. In *NMR Spectroscopy of Polymers*; Ibbett, R. N., Ed.; Blackie Academic & Professional: Glasgow, U.K., 1993; pp 275–307.
- (3) Schmidt-Rohr, K.; Spiess, H. W. *Multidimensional Solid-State NMR and Polymers*; Academic Press: London, 1994.
- (4) Seelig, J. *Q. Rev. Biophys.* **1977**, *10*, 353–418.
- (5) Davis, J. H. *Biochim. Biophys. Acta* **1983**, *737*, 117–171.
- (6) Mita, K.; Ichimura, S.; James, T. C. *J. Mol. Evol.* **1994**, *38*, 583–588.
- (7) Asakura, T.; Kaplan, D. L. In *Encyclopedia of Agricultural Science*; Arutzen, C. J., Ed.; Academic Press: London, 1994; Vol. 4, pp 1–11.
- (8) Saito, H.; Tabeta, R.; Asakura, T.; Iwanaga, Y.; Shoji, A.; Ozaki, T.; Ando, I. *Macromolecules* **1984**, *17*, 1405–1412.
- (9) Asakura, T.; Kuzuhara, A.; Tabeta, R.; Saito, H. *Macromolecules* **1985**, *18*, 1841–1845.
- (10) Ishida, M.; Asakura, T.; Yokoi, M.; Saito, H. *Macromolecules* **1990**, *23*, 88–94.
- (11) Asakura, T.; Demura, M.; Date, T.; Miyashita, N.; Ogawa, K.; Williamson, M. P. *Biopolymers* **1997**, *41*, 193–203.
- (12) Asakura, T.; Yeo, J. H.; Demura, M.; Itoh, T.; Fujito, T.; Imanari, M.; Nicholson, L. K.; Cross, T. A. *Macromolecules* **1993**, *26*, 6660–6663.
- (13) Nicholson, L. K.; Asakura, T.; Demura, M.; Cross, T. A. *Biopolymers* **1993**, *33*, 847–861.
- (14) Asakura, T.; Demura, M.; Hiraishi, Y.; Ogawa, K.; Uyama, A. *Chem. Lett.* **1994**, 2249–2252.
- (15) Asakura, T.; Demura, M. Manuscript in preparation.
- (16) Marsh, R. E.; Corey, R. B.; Pauling, L. *Biochim. Biophys. Acta* **1955**, *16*, 12–34.
- (17) Takahashi, Y.; Gehoh, M.; Yuzuriha, K. *J. Polym. Sci., Polym. Phys. Ed.* **1991**, *29*, 889–891.
- (18) Fossey, S. A.; Nemethy, G.; Gibson, K. D.; Scheraga, H. A. *Biopolymers* **1991**, *31*, 1529–1541.
- (19) Saito, H.; Tabeta, R.; Kuzuhara, A.; Asakura, T. *Bull. Chem. Soc. Jpn.* **1986**, *59*, 3383–3387.
- (20) Simmons, A. H.; Michal, C. A.; Jelinski, L. W. *Science* **1996**, *271*, 84–87.
- (21) Asakura, T.; Watanabe, Y.; Itoh, T. *Macromolecules* **1984**, *17*, 2421–2426.
- (22) Asakura, T.; Kawaguchi, Y.; Demura, M.; Osanai, M. *Insect Biochem.* **1988**, *18*, 531–538.
- (23) Asakura, T.; Yamada, H.; Demura, M.; Osanai, M. *Insect Biochem.* **1990**, *20*, 261–266.
- (24) Asakura, T.; Nagashima, M.; Sakaguchi, R.; Demura, M.; Osanai, M. *Insect Biochem.* **1991**, *21*, 743–748.
- (25) Asakura, T.; Sakaguchi, R.; Demura, M.; Manabe, T.; Uyama, A.; Ogawa, K.; Osanai, M. *Biotechnol. Bioeng.* **1993**, *41*, 245–252.
- (26) Asakura, T.; Yoshimizu, H.; Yoshizawa, F. *Macromolecules* **1988**, *21*, 2038–2041.
- (27) Yeo, J. H.; Demura, M.; Asakura, T.; Fujito, T.; Imanari, M.; Nicholson, L. K.; Cross, T. A. *Solid State NMR* **1994**, *3*, 209–218.
- (28) Asakura, T. *Makromol Chem.* **1981**, *182*, 1135–1145.
- (29) Kinsey, R. A.; Kimtanar, A.; Isai, M.-D.; Smith, R. J.; Janes, N.; Oldfield, E. *J. Biol. Chem.* **1981**, *256*, 4146–4149.
- (30) Ulrich, A. S.; Watts, A.; Wallat, I.; Heyn, M. P. *Biochemistry* **1994**, *33*, 5370–5375.
- (31) Ulrich, A. S.; Watts, A. *Solid State NMR* **1993**, *2*, 21–36.
- (32) Ulrich, A. S. *Macromol. Symp.* **1996**, *101*, 81–89.
- (33) Ulrich, A. S.; Wallat, I.; Heyn, M. P.; Watts, A. *Nature Struct. Biol.* **1995**, *2*, 190–192.
- (34) Asakura, T.; Demura, M.; Watanabe, Y.; Sato, K. *J. Polym. Sci., B* **1992**, *30*, 693–699.
- (35) Gall, C. M.; DiVerdi, J. A.; Opella, S. J. *J. Am. Chem. Soc.* **1981**, *103*, 5039–5043.
- (36) Saito, H.; Ishida, M.; Yokoi, M.; Asakura, T. *Macromolecules* **1990**, *23*, 83–87.
- (37) Lowenstein, J. M., Ed. *Citric Acid, Cycle, Control and Comportmentation*; Marcel Dekker: New York, 1969.

MA9616726